THE JOURNAL OF BIOLOGICAL CHEMISTRY VOL. 284, NO. 24, pp. 16531–16540, June 12, 2009

The *b* Subunits in the Peripheral Stalk of F_1F_0 ATP Synthase Preferentially Adopt an Offset Relationship*[S]

Received for publication, February 25, 2009, and in revised form, April 7, 2009 Published, JBC Papers in Press, April 15, 2009, DOI 10.1074/jbc.M109.002980

Shane B. Claggett[‡], **Mac O'Neil Plancher**[‡], **Stanley D. Dunn**[§], **and Brian D. Cain**[‡1]

From the [‡]*Department of Biochemistry and Molecular Biology, University of Florida, Gainesville, Florida 32605 and the* [§]*Department of Biochemistry, University of Western Ontario, London, Ontario N6A 5C1, Canada*

The peripheral stalk of F_1F_0 ATP synthase is essential for the binding of F_1 to F_O and for proper transfer of energy between the two sectors of the enzyme. The peripheral stalk of *Escherichia coli* is composed of a dimer of identical *b* subunits. In contrast, photosynthetic organisms express two *b*-like genes that form a heterodimeric peripheral stalk. Previously we generated chimeric peripheral stalks in which a portion of the tether and dimerization domains of the *E. coli b* subunits were replaced with homologous sequences from the *b* and *b′* subunits of *Thermosynechococcus elongatus* (Claggett, S. B., Grabar, T. B., Dunn, S. D., and Cain, B. D. (2007) *J. Bacteriol.* 189, 5463–5471). The spatial arrangement of the chimeric *b* and *b′* subunits, abbreviated *Tb* and *Tb′*, has been investigated by Cu^{2+}-mediated disulfide cross-link formation. Disulfide formation was studied both in soluble model polypeptides and between full-length subunits within intact functional F_1F_0 ATP synthase complexes. In both cases, disulfides were preferentially formed between Tb_{A83C} and Tb'_{A90C}, indicating the existence of a staggered relationship between helices of the two chimeric subunits. Even under stringent conditions rapid formation of disulfides between these positions occurred. Importantly, formation of this cross-link had no detectable effect on ATP-driven proton pumping, indicating that the staggered conformation is compatible with normal enzymatic activity. Under less stringent reaction conditions, it was also possible to detect *b* subunits cross-linked through identical positions, suggesting that an in-register, nonstaggered parallel conformation may also exist.

F_1F_0 ATP synthases are found in the inner mitochondrial membrane, the thylakoid membrane of chloroplasts, and the cytoplasmic membrane of bacteria (1–4). These enzymes are responsible for harnessing an electrochemical gradient of protons across the membranes for the synthesis of ATP. In *Escherichia coli* F_1F_0 ATP synthase, the membrane-embedded F_0 sector is composed of subunits ab_2c_{10} and a soluble F_1 portion composed of subunits $\alpha_3\beta_3\gamma\delta\epsilon$. The F_0 sector houses a proton channel located principally in the *a* subunit, and the flow of protons through F_0 generates torque used to rotate the c_{10} subunit ring relative to the ab_2 subunits. The F_1 γ and ϵ subunits are bound to the c_{10} ring and form the central or rotor stalk. Catalytic sites are located at the interfaces of each $\alpha\beta$ pair in F_1. The γ subunit extends into the center of the $\alpha_3\beta_3$ hexamer, creating an asymmetry in the conformations of the $\alpha\beta$ pairs (5). It is the rotation of the γ subunit and the resulting sequential conformational changes in each $\alpha\beta$ pair that provides the driving force for the synthesis of ATP at the catalytic sites. The $\alpha_3\beta_3$ hexamer is held stationary relative to the rotary stalk by the peripheral stalk consisting of the $b_2\delta$ subunits.

The peripheral stalk is essential for binding F_1 to F_0 and for coupling proton translocation to catalytic activity (6–8). In the *E. coli* enzyme, the peripheral stalk is a dimer of identical *b* subunits. The stalk has been conceptually divided into functional domains called the membrane domain ($b_{M1\text{-}I33}$), the tether domain ($b_{E34\text{-}A61}$), the dimerization domain ($b_{T62\text{-}K122}$), and the F_1-binding domain ($b_{Q123\text{-}L156}$) (9). Although there is ample evidence of direct protein-protein interactions between *b* subunits within the membrane, dimerization, and F_1-binding domains, there is remarkably little evidence of tight packing between the *b* subunits in the tether domain. In fact, electron spin resonance studies suggested that the tether domains of the two *b* subunits may be separated by more than 20 Å in the F_1F_0 complex (10, 11). Much of what is known about the structure of the stalk has been inferred from analysis of the properties of polypeptides modeling segments of the *b* subunit. The structure of a peptide modeling the membrane domain, $b_{M1\text{-}E34}$, has been determined by NMR (12), and a peptide based on the dimerization domain, $b_{T62\text{-}K122}$, has been determined by x-ray diffraction (13). Both polypeptides assumed α-helical conformations, but neither structure directly revealed *b* subunit dimerization interactions. Recently, Priya *et al.* (14) reported a low resolution structure of a $b_{M22\text{-}L156}$ dimer, but the extended conformation appears to be slightly too long to accurately reflect the dimensions of the peripheral stalk within the F_1F_0 complex.

Molecular modeling efforts supported by a variety of biochemical and biophysical experiments have yielded competing right-handed coiled coil (15, 16) and left-handed coiled coil (17, 18) models for the peripheral stalk. The parallel two-stranded left-handed coiled coli is a well known structure characterized by knobs-into-holes packing of the side chains of the two helices that are aligned in-register. An in-register conformation implies that any specific amino acid on the *b* subunit-subunit interface would occupy a position immediately adjacent to its counterpart in the other *b* subunit. In contrast, del Rizzo *et al.* (16) proposed a novel parallel right-handed coiled coil with the

* This work was supported by United States Public Health Service Grant GM70978 (to B. D. C.), a University of Florida Alumni Fellowship (to S. B. C.), and Canadian Institutes of Health Grant MOP-10237 (to S. D. D.).

[S] The on-line version of this article (available at http://www.jbc.org) contains supplemental Table S1.

[1] To whom correspondence should be addressed: Dept. of Biochemistry and Molecular Biology, Box 100245, University of Florida, Gainesville, FL 32610. Tel.: 352-392-6473; Fax: 352-392-2953; E-mail: bcain@biochem.med.ufl.edu.

helices of the two *b* subunits offset by approximately one and a half turns of an α helix. This staggered model positions the two identical residues contributed by each of the *b* subunits in a homodimer into differing environments and at considerable distance from one another. Sequence analyses have been offered in support of both models (16, 18). In terms of experimental support, cross-linking studies of polypeptides have provided evidence that dimer packing could be in-register at many sites starting from residue Ala[59] and continuing to the carboxyl termini in model $b_{Y24-L156}$ dimers and in $b_{D53-K122}$ dimers (9, 16). Cross-linking at a few of the carboxyl-proximal positions has been confirmed within intact F_1F_0 ATP synthase complexes (19, 20). Recent electron spin resonance distance measurements on b_{24-156} have also been interpreted as support for the in-register arrangement (17, 18). Conversely, work with polypeptides modeling the *b* subunit has generated evidence favoring a staggered conformation in this section of the dimer (15, 16, 21). In mixtures of dimerization domain polypeptides with cysteines incorporated at different sites, disulfides preferentially formed between positions that were 4–7 residues apart. For example, $b_{D53-L156}$ dimers were covalently locked into the offset conformation by the formation of disulfide bridges between cysteines introduced at positions b_{A79} and b_{R83} as well as b_{R83} and b_{A90} (15). These staggered dimers were more stable, melted with higher cooperativity, and bound soluble F_1 with higher affinity than $b_{D53-L156}$ dimers fixed in the in-register arrangement. Moreover, active and coupled F_1F_0 complexes were assembled with heterodimeric peripheral stalks using *b* subunits with tether domains varying in length by as many as 14 amino acids (22). These F_1F_0 complexes had peripheral stalks that were by definition out of register, at least within the tether domain.

In contrast to the homodimer of identical *b* subunits observed in the peripheral stalk of *E. coli*, photosynthetic organisms express two *b*-like subunits, *b* and *b′*, that are thought to form heterodimeric peripheral stalks in F_1F_0 ATP synthase. Previously, we generated heterodimeric peripheral stalks within the *E. coli* F_1F_0 by constructing chimeric *b* subunits (23). Segments of the tether and dimerization domains of the *E. coli b* subunit were replaced with the homologous regions of the *Thermosynechococcus elongatus b* and *b′* subunits. The chimeric subunits formed heterodimeric peripheral stalks that were incorporated into intact, functional F_1F_0 ATP synthase complexes. The most active chimeric enzymes had *T. elongatus* primary sequences replacing residues $b_{E39-I86}$ of the *E. coli b* subunit. For simplicity, these chimeric subunits will be referred to here as *Tb* and *Tb′*.

The ability to generate F_1F_0 ATP synthases with *Tb*/*Tb′* heterodimeric peripheral stalks provided a means to investigate the positions of the two subunits in the peripheral stalk. In the present work, we show that the *Tb* and *Tb′* subunits assumed preferred positions relative to one another within the F_1F_0 complex. The staggered conformation appears to be a favored and functional conformation for the peripheral stalk. However, within a population of F_1F_0 complexes, some complexes with peripheral stalks in the in-register conformation are likely to exist.

EXPERIMENTAL PROCEDURES

Bacterial Strains and Growth Conditions—The host strain for all membrane preparations was KM2 (Δ*b*), an *E. coli* strain that carries a chromosomal deletion of the *uncF* gene (*b* subunit) (24). Strain MM294 was used for the expression of peptides modeling the *b* subunit (25). F_1F_0 ATP synthase viability was assessed *in vivo* by growing cells on minimal A medium supplemented with succinate (0.2%, w/v). The cells for membrane preparations were grown in Luria broth supplemented with glucose (0.2%, w/v) and isopropyl-1-thio-β-D-galactopyranoside (40 μg/ml). Ampicillin (100 μg/ml) and chloramphenicol (25 μg/ml) were added as needed. All of the cells were grown at 37 °C.

Expression Plasmid Construction—A *b* subunit gene was synthesized by GenScript that contained a C21S mutation and a V5 epitope tag (GKPIPNPLLGLDST) on the carboxyl terminus. The C21S mutation is present in all *b*, *Tb*, and *Tb′* subunit gene constructs but will not be included in the subunit designations throughout the paper for clarity. Plasmid pSBC127 (b_{V5}) was generated by ligating the synthetic *uncF(b)* subunit gene from GenScript into the EcoRI/KpnI restriction sites of pUC19. Cysteine substitutions were engineered into *b* subunits by site-directed mutagenesis of plasmid pSBC127 (b_{V5}) using the oligonucleotides listed in supplemental Table S1. The plasmids were constructed for the expression of chimeric *Tb* or *Tb′* subunits with a cysteine substituted for residue Ala[83] or Ala[90] (see Table 1). *Tb* subunit substitutions were made in plasmid pSBC97 (Tb_{his}) that has *T. elongatus b* subunit sequence substituted for residues Glu[39]–Ile[86] and a histidine tag at the amino terminus. *Tb′* constructs were based on plasmid pSBC98 (Tb'_{V5}) that has the *T. elongatus b′* subunit sequence substituted for the same region and a V5 epitope tag on the carboxyl terminus. All of the mutations were confirmed by direct nucleotide sequencing.

Plasmids were also constructed to facilitate expression of soluble polypeptides modeled on the *Tb* and *Tb′* subunits (see Table 1). Regions of interest from the parent plasmids were amplified by PCR using the primers listed in supplemental Table S1 and cloned into the expression plasmid pJB3 (26) using the unique NdeI and HindIII sites. The forward primers for all of the *Tb* chimeras, SD101, and the *Tb′* chimeras, SD102, included an NdeI site and encoded a protein starting with residues MSY followed by *Tb* or *Tb′* sequence beginning at residue Asp[53]. Four plasmids were constructed to express peptides modeling the *Tb* or *Tb′* subunit residues Asp[53]–Leu[156] by PCR amplification of plasmids pSBC123 ($Tb_{E39-I86,A83C}$), pSBC124 ($Tb_{E39-I86,A90C}$), pSBC125 ($Tb'_{E39-I86,A83C}$) and pSBC126 ($Tb'_{E39-I86,A90C}$). Primers SD101/SD102 were used as the forward primer and SD104 as the reverse primer to generate plasmids pSD361 (Pb_{A83C}), pSD362 (Pb'_{A83C}), pSD363 (Pb_{A90C}), and pSD364 (Pb'_{A90C}), abbreviated as *Pb* and *Pb′*. Two additional plasmids expressing peptides modeling the *Tb* and *Tb′* dimerization domain residues Asp[53]–Lys[122] and containing a GGGC extension on the carboxyl terminus were constructed using SD103 as the reverse PCR primer and pSBC97 (*Tb*) or pSBC98 (*Tb′*) as the template DNA. The resulting plasmids pSD357 (Db_{+GGGC}) and pSD358 (Db'_{+GGGC}) are abbreviated as *Db* and *Db′*. Plasmid pSD357 (Db_{+GGGC}) was moved into the

expression plasmid pACT3 (27) using the EcoRI and HindIII sites to produce pSD359 (Db_{+GGGC}) and allow coexpression with pSD358 (Db'_{+GGGC}).

Preparation and Assay of Membranes—Membrane vesicles were prepared as described previously (28). Membrane protein concentrations were determined using the bicinchoninic acid method (29). ATP-driven proton pumping assays were conducted by adding 500 μg of membrane protein to 3.5 ml of reaction buffer (50 mM MOPS,[2] pH 7.3], 10 mM $MgCl_2$) and monitoring the fluorescence quenching of 9-amino-6-chloro-2-methoxyacridine (30). Fluorescence quenching was detected using a Photon Technologies International QuantaMaster 4 spectrofluorometer.

The ATP hydrolysis activities in membrane samples were determined using the 7-methyl-6-thioguanosine (MESG) method (31). This assay determines the rate of ATP hydrolysis by using the enzyme purine nucleotide phosphorylase (PNP) to catalyze the reaction of inorganic phosphate (P_i) with MESG to form 7-methyl-6-thioguanine. The appearance of product was detected as an absorbance increase at 360 nm using a Varian Cary 50 spectrophotometer. A PNP stock solution was made by dissolving the solid enzyme in water to a concentration of 0.1 units/ml and stored at 4 °C. An MESG stock solution was made in water to a final concentration of 1 mM and stored in 5-ml aliquots at −20 °C. The MESG solution was thawed prior to use, and both MESG and PNP were kept on ice until needed. Each reaction consisted of 10–25 mg of membrane protein, 50 ml of 20× TM buffer (1 M Tris-HCl, pH 7.5, 200 mM $MgSO_4$), 300 ml of MESG, 50 ml of PNP, and water to a final volume of 1 ml. The components were combined in a disposable glass tube, agitated briefly to mix, and poured into a cuvette prewarmed to 37 °C. Each reaction was allowed to sit for 1 min to stabilize the temperature before starting by the addition of 30 ml of 0.15 M ATP made in TM buffer. Absorbance data points were collected continuously for 5 min. The slope of the linear portion of the reaction was determined in units of absorbance/min using the software associated with the instrument. Stimulation of ATP hydrolysis by *N*,*N*-dimethyldodecylamine *N*-oxide (LDAO) was determined by adding LDAO to each reaction to a final concentration of 0.5% as described previously (32).

Heterodimeric peripheral stalks were detected using a purification procedure essentially as described previously (22). Membrane samples were solubilized and purified over a high capacity nickel chelate affinity matrix (Sigma) to selectively retain F_1F_0 ATP synthase complexes containing at least one histidine tag. Membrane- and nickel resin-purified proteins were separated on a 15% SDS-PAGE gel for immunoblot analysis (33). Primary antibodies used were an antibody against the *b* subunit (a gift from G. Deckers-Hebestreit) and an antibody against the V5 epitope tag (Invitrogen). Secondary antibodies used were horseradish peroxidase-linked anti-rabbit and anti-mouse antibodies, respectively. The presence of bound secondary antibody was detected by chemiluminescence with the Amersham Biosciences ECL Plus Western blotting detection system.

Expression and Purification of Soluble b Subunits—The chimeric dimerization domains Db_{+GGGC} and Db'_{+GGGC} were coexpressed by isopropyl-1-thio-β-D-galactopyranoside induction in cells carrying both pSD359 (Db_{+GGGC}) and pSD359 (Db'_{+GGGC}). The *Tb* and *Tb′* chimeras were separated by ion exchange chromatography, exploiting their substantial difference in charge. The cell extracts were first fractionated by procedures similar to those that have been previously described (16) and then clarified by ultracentrifugation. Proteins that precipitated with ammonium sulfate at concentrations between 40 and 60% of saturation were collected. Anion exchange chromatography on DEAE-Sepharose at pH 8.0 separated the domains into two peaks. Further fractionation of the first peak by cation exchange chromatography on SP-Sepharose at pH 5.0 yielded essentially pure *Tb* dimerization domain. Application of the cation exchange step to the second peak resulted in partially purified *b′* chimera; subsequent size exclusion chromatography on a column of Sephadex G-75 yielded the pure polypeptide. Chimeric polypeptides consisting of residues Asp^{53}–Leu^{156} and containing internal cysteine substitutions at either position Ala^{83} or Ala^{90} were expressed by isopropyl-1-thio-β-D-galactopyranoside induction of cells carrying plasmids pSD361, pSD362, pSD363, or pSD364. Following cell breakage and clarification of the extracts by ultracentrifugation, the supernatant solutions were brought to 45% saturation with ammonium sulfate. The precipitates were collected by centrifugation, dissolved, and dialyzed against 50 mM Tris-HCl, pH 7.5, containing 1 mM EDTA and 1 mM dithiothreitol. These partially purified samples were used for disulfide formation studies without further purification. The identity and purity of each product was confirmed by matrix-assisted laser desorption ionization time-of-flight mass spectrometry; the masses of the *Tb* and *Tb′* subunits differ by 167 Da. All of the buffers included dithiothreitol to a final concentration of 1 mM to maintain the cysteines in a reduced state. Protein concentrations were determined by the Advanced Assay (Cytoskeleton, Inc.) as described previously (16). Purified proteins were analyzed on 15% SDS-PAGE gels using a Tris-Tricine buffer system (9).

Disulfide Cross-linking—Disulfide cross-links between *b* subunits in the peripheral stalk were formed by incubating membrane samples with 50 mM Cu^{2+} for time periods specified for each experiment. The cross-linking reactions were carried out in open 1.5-ml microcentrifuge tubes with mixing at 300 rpm in an Eppendorf Thermomixer R heated to 37 °C. Each reaction was stopped by adding fresh *N*-ethylmaleimide (NEM) to a final concentration of 5 mM, through mixing and cooling on ice. Two time points were taken for each sample, a zero time point and a 2- or 10-min time point. The zero time point sample was obtained by diluting the concentrated membranes to 5 mg/ml in TM buffer and adding NEM to react with free cysteine residues and prevent cross-linking. The reaction was mixed and allowed to sit at room temperature for 15 s before adding Cu^{2+} and placing on ice. Cross-linking for 2 or 10 min was done by diluting the membrane sample to 5 mg/ml in TM buffer and warming to 37 °C in the thermomixer. Prewarmed Cu^{2+} was added, and the samples were allowed to incubate with mixing

[2] The abbreviations used are: MOPS, morpholinepropanesulfonic acid; LDAO, *N*,*N*-dimethyldodecylamine *N*-oxide; MESG, 7-methyl-6-thioguanosine; NEM, *N*-ethylmalemide; PNP, purine nucleotide phosphorylase; Tricine, *N*-[2-hydroxy-1,1-bis(hydroxymethyl)ethyl]glycine.

TABLE 1
Growth of bacterial strains

Strain/plasmid(s)	Gene product[a–e]	Antibiotic resistance[f]	Growth on succinate[g]	Source or reference
KM2/pTAM37/pTAM46	b_{his}/b_{V5}	Ap+Cm	+++	Ref. 22
KM2/pBR322	Δb	Ap	−	New England Biolabs
KM2/pSBC127	b_{V5}	Ap	++	This study
KM2/pSBC128	$b_{I76C, V5}$	Ap	++	This study
KM2/pSBC129	$b_{R83C, V5}$	Ap	++	This study
KM2/pSBC130	$b_{A90C, V5}$	Ap	++	This study
KM2/pSBC131	$b_{E97C, V5}$	Ap	+	This study
KM2/pSBC97	*Tb*	Cm	+	[23]
KM2/pSBC123	Tb_{A83C}	Cm	+	This study
KM2/pSBC124	Tb_{A90C}	Cm	+	This study
KM2/pSBC98	*Tb′*	Ap	++	[23]
KM2/pSBC125	Tb'_{A83C}	Ap	++	This study
KM2/pSBC126	Tb'_{A90C}	Ap	++	This study
KM2/pSBC97/pSBC98	*Tb*/*Tb′*	Ap + Cm	++	[23]
KM2/pSBC123/pSBC125	Tb_{A83C}/Tb'_{A83C}	Ap + Cm	++	This study
KM2/pSBC123/pSBC126	Tb_{A83C}/Tb'_{A90C}	Ap + Cm	++	This study
KM2/pSBC124/pSBC125	Tb_{A90C}/Tb'_{A83C}	Ap + Cm	+	This study
KM2/pSBC124/pSBC126	Tb_{A90C}/Tb'_{A90C}	Ap + Cm	++	This study
MM294/pSD359	Db_{+GGGC}	Cm	N/A	This study
MM294/pSD358	Db'_{+GGGC}	Ap	N/A	This study
MM294/pSD361	Pb_{A83C}	Ap	N/A	This study
MM294/pSD363	Pb_{A90C}	Ap	N/A	This study
MM294/pSD362	Pb'_{A83C}	Ap	N/A	This study
MM294/pSD364	Pb'_{A90C}	Ap	N/A	This study

[a] *Tb*, wild-type *E. coli b* subunit with sequence from the *b* subunit of *T. elongatus* substituted for amino acids Glu^{39}–Ile^{86}, a C21S mutation, and a six-histidine epitope tag at the amino terminus.
[b] *Tb′*, wild-type *E. coli b* subunit with sequence from the *b′* subunit of *T. elongatus* substituted for amino acids Glu^{39}–Ile^{86}, a C21S mutation, and a V5 epitope tag (GKPIPNPLLGLDST) at the carboxyl terminus.
[c] The native cysteine at b_{C21} has been mutated to serine in all pSBC plasmids.
[d] The *Db* and *Db′* genes produce peptides modeling the dimerization domains of the *Tb* and *Tb′* subunits. These peptides have the sequence MSY at the amino terminus, contain *Tb*/*Tb′* residues Asp^{53}–Lys^{122} in the middle, and terminate with the sequence GGGC at the carboxyl terminus.
[e] The *Pb* and *Pb′* genes produce peptides modeling the D53-L156 regions of the *Tb* and *Tb′* subunits. These peptides also start with the sequence MSY and have cysteine residues substituted at either Ala^{83} or Ala^{90} as specified.
[f] Ap, ampicillin; Cm, chloramphenicol.
[g] +++, wild-type growth; ++, colonies smaller than wild-type; +, small colony formation; −, no growth.

for 2 or 10 min before further cross-linking was stopped by the addition of NEM. A total of 1 μg of each cross-linked sample was analyzed by Western blot using an antibody against the V5 epitope tag. Each band in the Western blot was quantified using the program UN-SCAN-IT (Silk Scientific).

Soluble b Subunit Cross-linking—The propensity of the soluble *Tb* and *Tb′* dimerization domains with carboxyl-terminal GGGC (Db_{GGGC} and Db'_{GGGC}) additions to form homodimers and heterodimers was determined by dialysis of either individual polypeptides, or an equimolar mixture of the *Tb* and *Tb′* constructs, overnight at 4 °C against buffer containing 50 mM sodium phosphate, 10 μM $CuCl_2$, and cysteine at concentrations of 0, 1, or 10 mM. The total protein concentration was 0.5 mg/ml in each case. The samples were treated with SDS sample buffer containing NEM to prevent further cross-link formation. The tendency of chimeric polypeptides consisting of residues Asp^{53}–Leu^{156} and containing internal cysteine substitutions at either residue Ala^{83} or Ala^{90} to form disulfide cross-links was assessed by dilution of partially purified protein samples, or mixtures, into a sulfhydril/disulfide buffer prepared by the addition of 10 mM β-mercaptoethanol and 2.5 mM dithiobisnitrobenzoate to 50 mM Tris-HCl buffer, pH 7.4. Following incubation at 25 °C for 30 min, the samples were treated with SDS sample buffer containing 15 mM NEM to prevent further cross-link formation.

RESULTS

Cysteine Substitutions in the E. coli b Subunit—A plasmid carrying a synthetic cysteine-less *b* subunit gene equipped with a carboxyl-terminal V5 epitope tag (b_{V5}) was generated to facilitate construction and expression of recombinant subunits. To look for evidence of an in-register conformation in the dimerization domain of the peripheral stalk of the *E. coli* F_1F_0 ATP synthase, four mutations were constructed within the synthetic gene for expression of cysteine substitution subunits $b_{I76C,V5}$, $b_{R83C,V5}$, $b_{A90C,V5}$, and $b_{E97C,V5}$ (Table 1). These positions were selected based on earlier work with model polypeptides (16). Each of the new plasmids was transformed into strain *E. coli* strain KM2 (Δb). Complementation of the strain was examined by growth on minimal A medium supplemented with succinate. The succinate growth experiments indicated that all cysteine insertion *b* subunits were functionally incorporated into F_1F_0 ATP synthase complexes (Table 1). However, it should be noted that the colonies of KM2/pSBC127 (b_{V5}) expressing the synthetic *uncF(b)* gene were typically smaller than a strain with the epitope tags added to native *uncF(b)* genes. Subsequent inclusion of the cysteine substitution mutations had no further discernable effect on growth.

The membranes from each strain were prepared and studied for ATP hydrolysis activity in both the absence of presence of 0.5% LDAO as a measure of the relative amounts of intact F_1F_0 complexes (Table 2). Membranes from KM2/pSBC128 ($b_{I76C,V5}$) had only two-thirds of the activity seen in the positive control membranes, but F_1F_0-ATPase activities in the other cysteine mutation membrane samples were not statistically different from values obtained for control KM2/pTAM37/pTAM46 (b_{his}/b_{V5}) membranes. The extent of coupling between ATP hydrolysis at F_1 and proton pumping at F_0 was quantified using a fluorescence-based ATP-driven proton

TABLE 2
ATP hydrolysis activity of engineered F_1F_0

Strain/Plasmid(s)	Gene product[a]	ATP hydrolysis[b]		Fold induction
		−LDAO	+LDAO[c]	
KM2/pTAM37/pTAM46	b_{his}/b_{V5}	0.30 ± 0.02	1.2 ± 0.06	4.0
KM2/pBR322	Δb	0.07 ± 0.01	0.2 ± 0.01	2.3
KM2/pSBC127	b_{V5}	0.29 ± 0.01	1.3 ± 0.08	4.4
KM2/pSBC128	$b_{I76C, V5}$	0.19 ± 0.01	0.9 ± 0.03	4.6
KM2/pSBC129	$b_{R83C, V5}$	0.28 ± 0.07	1.2 ± 0.07	4.3
KM2/pSBC130	$b_{A90C, V5}$	0.29 ± 0.04	1.2 ± 0.11	4.0
KM2/pSBC131	$b_{E97C, V5}$	0.33 ± 0.07	1.1 ± 0.07	3.4
KM2/pSBC97	*Tb*	0.30 ± 0.02	1.0 ± 0.15	3.4
KM2/pSBC123	Tb_{A83C}	0.19 ± 0.03	0.7 ± 0.05	3.7
KM2/pSBC124	Tb_{A90C}	0.20 ± 0.04	0.7 ± 0.06	3.5
KM2/pSBC98	*Tb′*	0.17 ± 0.02	0.5 ± 0.06	2.9
KM2/pSBC125	Tb'_{A83C}	0.10 ± 0.01	0.2 ± 0.01	2.2
KM2/pSBC126	Tb'_{A90C}	0.10 ± 0.01	0.2 ± 0.01	2.3
KM2/pSBC97/pSBC98	*Tb*/*Tb′*	0.24 ± 0.02	0.9 ± 0.04	3.7
KM2/pSBC123/pSBC125	Tb_{A83C}/Tb'_{A83C}	0.19 ± 0.01	0.6 ± 0.01	3.2
KM2/pSBC123/pSBC126	Tb_{A83C}/Tb'_{A90C}	0.23 ± 0.02	0.8 ± 0.02	3.4
KM2/pSBC124/pSBC125	Tb_{A90C}/Tb'_{A83C}	0.19 ± 0.02	0.7 ± 0.05	3.8
KM2/pSBC124/pSBC126	Tb_{A90C}/Tb'_{A90C}	0.21 ± 0.02	0.8 ± 0.07	3.6

[a] See Table 1 for gene product definitions.
[b] Reported in μmol of P_i/mg of membrane protein/min.
[c] Used to release F_1 from the inhibitory effect of F_0.

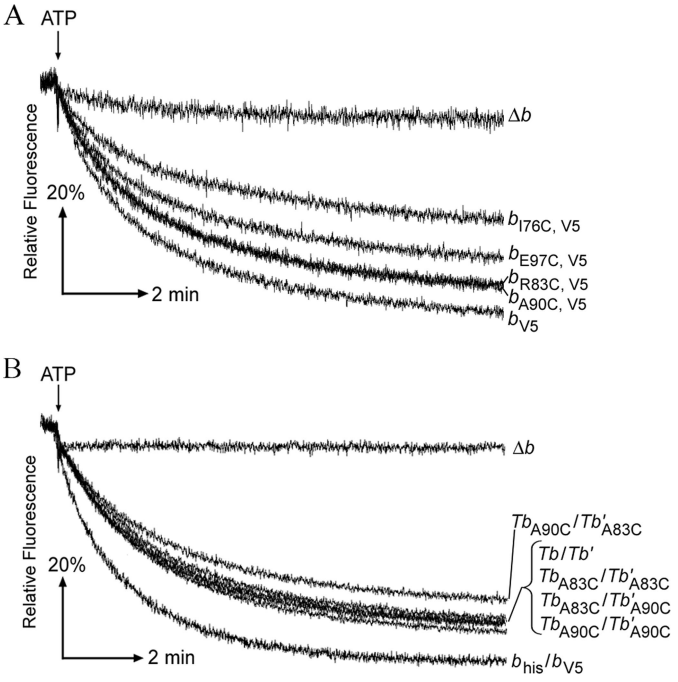

FIGURE 1. **Effects of *b* subunit engineering on enzyme coupling as measured by ATP-driven energization of inverted membrane vesicles (34).** Membranes prepared from strains KM2/pTAM37/pTAM46 (b_{his}/b_{V5}) and KM2/pBR322 (Δ*b*) were used as positive and negative controls, respectively. The point where ATP was added is indicated above each graph, and the expressed *b* subunits are listed on the *right*. The traces were obtained in triplicate using a Photon Technologies International spectrofluorimeter, and the results shown are individual representative results. *A*, traces shown are from membranes prepared from strains KM2/pSBC127 (b_{V5}), KM2/pSBC128 ($b_{I76C,V5}$), KM2/pSBC129 ($b_{R83C,V5}$), KM2/pSBC130 ($b_{A90C,V5}$), and KM2/pSBC131 ($b_{E97C,V5}$). *B*, traces shown are from membranes prepared from strains KM2/pSBC97 (*Tb*), KM2/pSBC123 (Tb_{A83C}), KM2/pSBC124 (Tb_{A90C}), KM2/pSBC98 (*Tb′*), KM2/pSBC125 (Tb'_{A83C}), KM2/pSBC126 (Tb'_{A90C}), KM2/pSBC97/pSBC98 (*Tb*/*Tb′*), KM2/pSBC123/pSBC125 (Tb_{A83C}/Tb'_{A83C}), KM2/pSBC123/pSBC126 (Tb_{A83C}/Tb'_{A90C}), KM2/pSBC124/pSBC125 (Tb_{A90C}/Tb'_{A83C}), and KM2/pSBC124/pSBC126 (Tb_{A90C}/Tb'_{A90C}).

pumping assay (Fig. 1*A*). Although very significant levels of coupled activity were evident in all of the samples, the *b* subunit cysteine substitution membranes had somewhat reduced proton pumping activity. As might be expected, strain KM2/pSBC128 ($b_{I76C,V5}$) membranes showed the most significant reduction, with only ~50% of activity found in KM2/pSBC127 (b_{V5}) membranes. Nevertheless, all four cysteine substitution *b* subunits supported enzyme complex assembly and provided readily detectable levels of F_1F_0 ATP synthase activity.

Evidence for an In-register Parallel Peripheral Stalk—The approach to looking for an in-register conformation for *b* subunits within the peripheral stalk was straightforward. In these experiments, *E. coli b* subunits with the single cysteine substitutions were expressed forming a homodimeric peripheral stalk. Disulfide cross-link formation was induced by treating membranes prepared from strains expressing subunits b_{V5}, $b_{I76C,V5}$, $b_{R83C,V5}$, $b_{A90C,V5}$, or $b_{E97C,V5}$ for 2 min with high concentrations (500 μM) of the oxidizing agent $CuCl_2$. Levels of monomeric and cross-linked dimeric subunits were determined by Western blot analysis using an antibody against the V5 epitope tag (Fig. 2*A*). Analysis of multiple experiments revealed that ~70% of the $b_{A90C,V5}$ subunits could be cross-linked. Only 20–25% of the $b_{R83C,V5}$ and $b_{E97C,V5}$ subunits were cross-linked, and very little if any cross-link formation was detectable in the $b_{I76C,V5}$ sample. The results provided additional evidence of the existence of an in-register conformation of the peripheral stalk in intact F_1F_0 ATP synthase. To test whether the disulfide cross-links were capable of forming under more selective conditions, the oxidizing agent concentration was lowered to 50 μM, and the reaction time was increased to 10 min. No apparent dimer formation was observed with cysteine substitutions at b_{I76C}, b_{R83C}, b_{A90C}, or b_{E97C} (Fig. 2*B*). Therefore, even the most efficient cross-link observed in the homodimeric $b_{A90C,V5}/b_{A90C,V5}$ peripheral stalk was not detectable under more stringent reaction conditions.

Cross-linking in Tb and Tb′ Polypeptides—Cross-linking in the *E. coli b* subunits produced evidence supporting an in-register model for the peripheral stalk, but the staggered model cannot be readily tested in a homodimeric stalk because the two *b* subunits are indistinguishable from each other. Hence, we took advantage the heterodimeric chimeric *Tb/Tb′* subunit

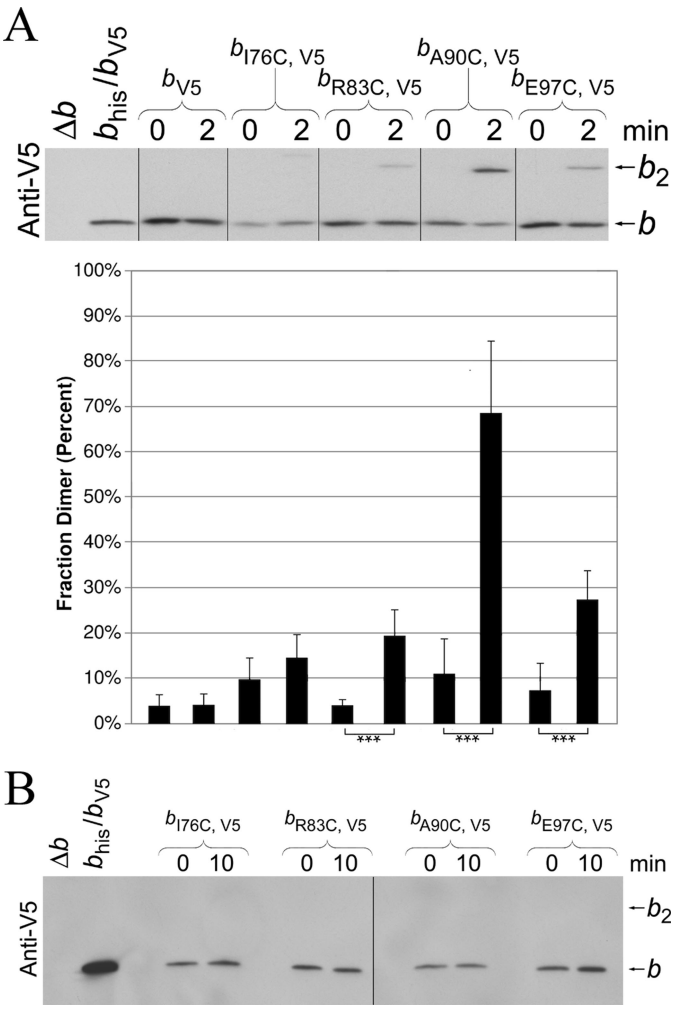

FIGURE 2. **Disulfide cross-link formation in F_1F_0 ATP synthase complexes containing engineered *E. coli* peripheral stalks.** *A*, membranes were prepared in the presence of 5 mM Tris (2-carboxyethyl) phosphine from strains KM2/pSBC127 (b_{V5}), KM2/pSBC128 ($b_{I76C,V5}$), KM2/pSBC129 ($b_{R83C,V5}$), KM2/pSBC130 ($b_{A90C,V5}$), and KM2/pSBC131 ($b_{E97C,V5}$). Cross-link formation was induced by diluting samples to 5 mg/ml and adding Cu^{2+} to a final concentration of 500 μM. The reactions were carried out at 37 °C with shaking for 2 min, and the cross-linking reaction was quenched by adding NEM. The fraction dimer was calculated for each sample by dividing the dimer band by the sum of the monomer and dimer bands. The *vertical lines* indicate the removal of intervening lanes from the gel *in silico*. The samples with a low probability of being identical are indicated (*, $p < 0.05$; **, $p < 0.01$; ***, $p < 0.001$; $n = 6$). *B*, samples were prepared and cross-linked essentially as described for *A* with the exception that the Cu^{2+} concentration was reduced to 50 μM, and the reaction time was increased to 10 min.

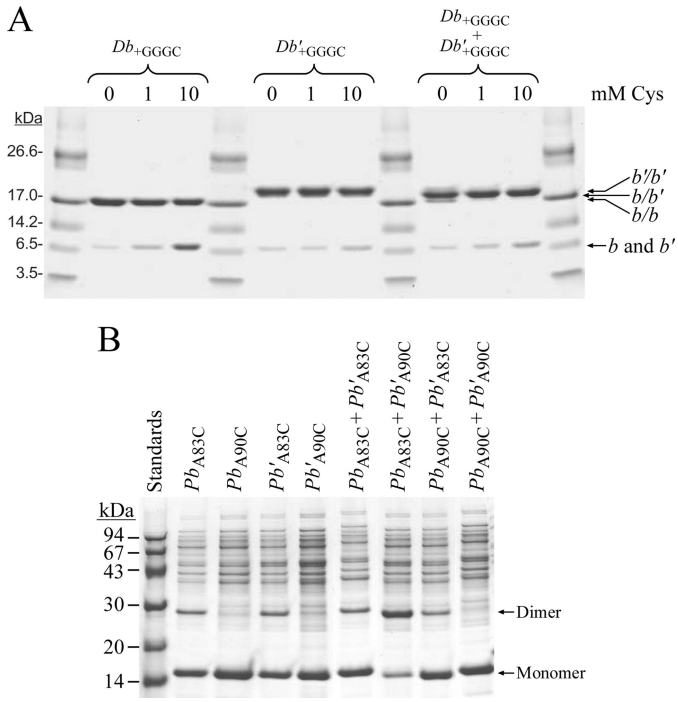

FIGURE 3. **Disulfide cross-linking of peptide fragments modeling the chimeric *Tb* and *Tb′* subunits.** *A*, the propensity of peptides modeling the dimerization domain of chimeric *Tb* and *Tb′* subunits and containing carboxyl-terminal GGGC extensions to form homodimeric and heterodimeric arrangements was investigated using disulfide cross-link formation. The peptide fragments Db_{+GGGC} and Db'_{+GGGC} were purified from strain MM294/pSD359/pSD358 (Db_{+GGGC}/Db'_{+GGGC}) as described under "Experimental Procedures." The location of the chimeric *b* and *b′* subunits, both monomeric and dimeric, are labeled on the *right side* of the gel. Assignment of the dominant species was confirmed by mass spectrometry. *B*, disulfide cross-link formation between cysteines substituted at residues Ala^{83} or Ala^{90} in peptides modeling the dimerization and F_1-binding domains of the chimeric subunits was analyzed by SDS-PAGE. Peptides from strains MM294/pSD361 (Pb_{A83C}), MM294/pSD362 (Pb'_{A83C}), MM294/pSD363 (Pb_{A90C}), and MM294/pSD364 (Pb'_{A90C}) were purified as described under "Experimental Procedures." The proteins were diluted individually or in combination into a sulfhydril/disulfide buffer and incubated at 25 °C for 30 min. The cross-linking reaction was terminated by treated with SDS sample buffer containing 15 mM NEM, and each sample was analyzed by SDS-PAGE. The positions of the monomeric and dimeric bands are indicated on the *right side* of the gel.

enzyme (20) to devise a specific test of the staggered conformation hypothesis.

To correlate the properties of *Tb* and *Tb′* with the extensive work on polypeptides modeling the native *E. coli b* subunit, the dimerization domains containing residues $b_{D53\text{-}K122}$ of the *Tb* and *Tb′* subunits were expressed and purified to homogeneity. Circular dichroism spectra of both forms and of mixtures exhibited strong minima at 208 and 222 nm (data not shown), implying that the chimeric peptides could form both homodimers and heterodimers. To determine whether formation of heterodimer was favored, the dimerization domains were expressed with carboxyl-terminal GGGC additions. A previous study (16) using the *E. coli* dimerization domain showed that disulfide formation between the added GGGC extensions produced stably linked dimers without perturbing the size and shape of the native structure. Disulfide formation tests were conducted on the individual polypeptides and mixtures using Cu^{2+}-mediated oxidation in the presence of various levels of free cysteine to provide specificity (Fig. 3*A*). In the absence of any cysteine, both individual domains formed disulfides effectively. The reduced forms of the domains migrated identically, but the disulfide-linked $(Db_{+GGGC})_2$ dimer was distinguished from the $(Db'_{+GGGC})_2$ dimer by a difference in migration speed. The prominent product obtained with an equimolar mixture of the two domains showed an intermediate mobility and was assigned as the Db_{+GGGC}/Db'_{+GGGC} heterodimer. The specificity of dimer formation in this experiment can be increased by the addition of free cysteine to the buffer, because peptidyl cysteines that are not located proximal to a partner peptidyl cysteine are more likely to make a mixed disulfide with the free cysteine. The addition of 10 mM cysteine increased the specificity of heterodimer formation in the mixture. These results imply that each of the individual chimeric

peptides was capable of forming homodimers under the conditions of the experiment but that the formation of heterodimers was favored in mixtures because of the *T. elongatus* portion of the sequence.

The specificity of disulfide formation between cysteines substituted for residues Ala^{83} and Ala^{90} was tested using soluble forms of the chimeric subunits that consisted of residues $b_{D53–L156}$ (Fig. 3*B*). Partially purified peptides were incubated, either individually or as mixtures, for 30 min in a thiol-disulfide buffer and analyzed by nonreducing SDS-PAGE. Both the individual homodimeric $(Pb_{A83C})_2$ and $(Pb'_{A83C})_2$ polypeptides and the mixture of them both showed modest tendencies to form disulfides, whereas no dimer formation was observed for either of the individual constructs with cysteine at position 90. Of all the possible cross-linking arrangements tested, dimer formation was found to be the strongest in the Pb_{A83C}/Pb'_{A90C} mixture, implying a proximity for position 83 of *Pb* and position 90 of *Pb′*. Dimer formation for the Pb_{A90C}/Pb'_{A83C} peptide mixture was substantially weaker. Importantly, the *T. elongatus* sequences appeared to be dictating positioning of the chimeric peptides relative to one another.

Evidence for a Staggered Parallel Peripheral Stalk—Plasmids were constructed to express the chimeric $Tb_{his,A83C}$, $Tb_{his,A90C}$, $Tb'_{A83C,V5}$, and $Tb'_{A90C,V5}$ subunits. The chimeric subunits were expressed in deletion strain KM2 (Δ*b*) individually and in combination and then assayed for *in vivo* F_1F_0 activity by growth on succinate as the sole carbon source. All of the cysteine-containing subunits complemented the deletion strain and supported colony formation comparable with the unmodified chimeric subunits (Table 1). The membranes were prepared from the paired chimeric subunit samples and analyzed for ATP hydrolysis activity in both the absence and the presence of 0.5% LDAO (Table 2). All four combinations of A83C and A90C chimeric subunits yielded membrane vesicles with activities approaching levels found in control KM2/pSBC97/pSBC98 (Tb_{his}/Tb'_{V5}) membranes. Analysis of enzyme coupling using the proton pumping assay indicated that the cysteine insertion subunits produced no significant effect on coupling (Fig. 1*B*).

The levels of disulfide formation in F_1F_0 ATP synthase peripheral stalks were examined in membranes prepared from the strains expressing both chimeric *Tb* and *Tb′* subunits. The initial experiments were conducted by cross-linking under high Cu^{2+} concentration conditions (Fig. 4, *A* and *B*). Cross-linking was evident in membranes containing all four chimeric subunit combinations: $Tb_{his,A83C}/Tb'_{A83C,V5}$, $Tb_{his,A83C}/Tb'_{A90C,V5}$, $Tb_{his,A90C}/Tb'_{A83C,V5}$, and $Tb_{his,A90C}/Tb'_{A90C,V5}$. Interpretation of the experiment was complicated because each sample contained a mixture of F_1F_0 complexes with heterodimeric *Tb/Tb′* stalks and homodimeric *Tb/Tb* and *Tb′/Tb′* peripheral stalks. Membranes prepared from strains expressing a pair of chimeric subunits where only one type of subunit contained a cysteine substitution produced a significant degree of cross-link formation (Fig. 4*C*), indicating that homodimeric peripheral stalks likely contributed to the total cross-linked product observed in the membrane fractions where both subunits contained cysteines. Therefore, to detect only cross-link formation specifically attributable to heterodimeric peripheral stalks, each sample was purified over a nickel resin after cross-linking and analyzed by Western blot using an antibody against the V5 epitope tag (Fig. 4*D*). Strong dimer formation was observed for both the $Tb_{his,A90C}/Tb'_{A90C,V5}$ and $Tb_{his,A83C}/Tb'_{A90C,V5}$ peripheral stalks. The data set cannot be easily reconciled with respect to either an exclusively in-register conformation or an exclusively staggered conformation but arguably offers support for both competing models. It should be noted that the cross-linked $Tb_{his,A90C}/Tb'_{A83C,V5}$ peripheral stalk was barely detectable in comparison with the $Tb_{his,A83C}/Tb'_{A90C,V5}$. The result was in accord with the apparent orientation of the stagger observed in the polypeptide work (Fig. 3*B*). Together the evidence indicates that the chimeric subunits assume preferred and distinguishable positions within the heterodimeric stalks. The evidence further supports a staggered conformation within the dimerization domain that has the *Tb* subunits offset in the carboxyl direction with respect to the *Tb′* subunit.

The Cu^{2+} concentration was reduced to 50 μM to more selectively form only those cross-links that occur with the highest efficiency (Fig. 5*A*). Higher concentrations of Cu^{2+} inhibited F_1F_0 ATPase, but 50 μM Cu^{2+} allowed for direct measurement of enzymatic activity. Under these conditions the only sample that was successfully cross-linked contained $Tb_{his,A83C}/Tb'_{A90C,V5}$ peripheral stalks. The dimer band observed was the cross-linked product of $Tb_{his,A83C}/Tb'_{A90C,V5}$ heterodimer F_1F_0 complex and not cross-linking in a homodimeric stalk, a fact that can be deduced from the lack of dimer formation in samples expressing either $Tb_{his,A83C}$ and $Tb_{his,A83C}$ subunits or $Tb'_{A90C,V5}$ and $Tb'_{A90C,V5}$ subunits. A reaction time course study showed that the Tb_{A83C}/Tb'_{A90C} cross-linking reached its maximum within 40 s (Fig. 5*B*). Image analysis of the Western blots indicated that ~70% of the Tb'_{A90C} subunit was paired with a Tb_{A83C} subunit and cross-linked upon treatment with oxidizing agent. Indeed, the zero time point samples show a degree of background cross-link formation occurring even in the presence of the Tris (2-carboxyethyl) phosphine reducing agent. Clearly, the rapid, high efficiency $Tb_{his,A83C}/Tb'_{A90C,V5}$ cross-linking was reporting on an offset structure extant in the peripheral stalk, and not less than two-thirds of the peripheral stalks were in a staggered rather than in-register conformation.

If it were necessary to revert to an in-register conformation for enzyme function, then trapping 70% of the enzyme in the stagger by disulfide bridge formation would be expected to have a readily detectable impact on activity. The effect of cross-link formation on coupled enzyme activity was analyzed using the proton pumping assay (Fig. 5*C*). Importantly, the formation of this cross-link had no effect on enzyme coupling, demonstrating that a peripheral stalk covalently locked in the offset arrangement represented a fully functional form of the enzyme.

DISCUSSION

The goal of this study was to provide direct tests of two competing structural models of the peripheral stalk of F_1F_0 ATP synthase. One model proposed that the *b* subunits are in a staggered parallel conformation (15, 16, 21), and the other suggested an in-register parallel arrangement (9, 19, 20). We have provided evidence compatible with both conformations, but the staggered positions appeared to be highly preferred. The

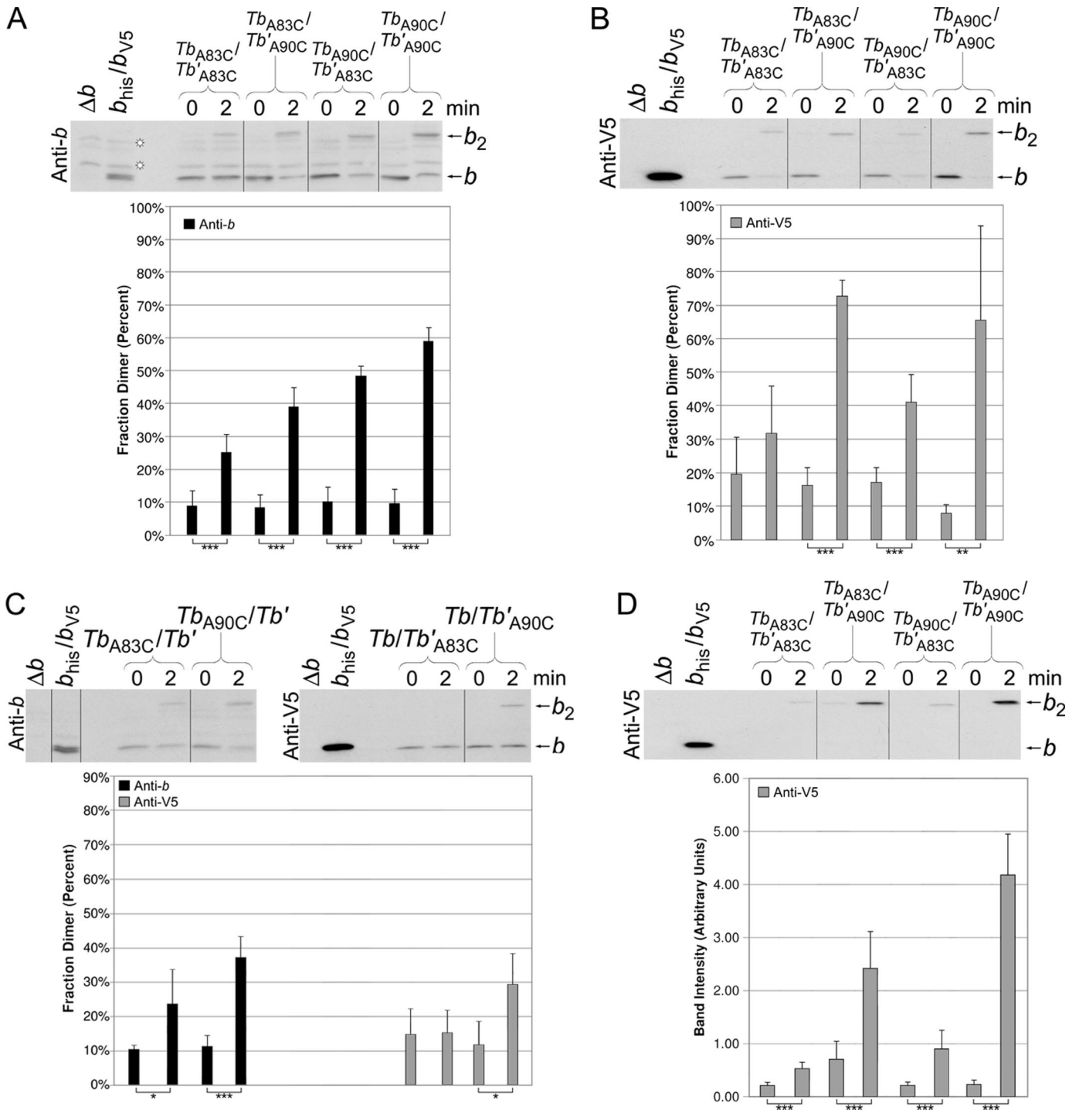

FIGURE 4. **Disulfide cross-link formation in F_1F_0 ATP synthase peripheral stalks composed of chimeric *Tb* and *Tb′* subunits.** The membranes were prepared from strains coexpressing cysteine-containing *Tb* and *Tb′* subunits. Samples from KM2/pSBC123/pSBC125 (Tb_{A83C}/Tb'_{A83C}), KM2/pSBC123/pSBC126 (Tb_{A83C}/Tb'_{A90C}), KM2/pSBC124/pSBC125 (Tb_{A90C}/Tb'_{A83C}), and KM2/pSBC124/pSBC126 (Tb_{A90C}/Tb'_{A90C}) were cross-linked with 500 μM Cu^{2+} exactly as described for Fig. 2 and analyzed by Western blot using antibodies against the *b* subunit (*A*) and V5 epitope tag (*B*) (10 and 1 μg of protein/lane, respectively). The *vertical lines* indicate the removal of intervening lanes *in silico*. Samples with a low probability of being identical are indicated (*, $p < 0.05$; **, $p < 0.01$; ***, $p < 0.001$; $n = 5$). *C*, membranes were prepared from strains coexpressing a cysteine-containing chimeric subunit with the complementary cysteine-free chimeric subunit. Samples from KM2/pSBC123/pSBC98 (Tb_{A83C}/Tb'), KM2/pSBC124/pSBC98 (Tb_{A90C}/Tb'), KM2/pSBC97/pSBC125 (Tb/Tb'_{A83C}), and KM2/pSBC97/pSBC126 (Tb/Tb'_{A90C}) were cross-linked as before and analyzed by Western blot. Antibodies against either the *b* subunit or the V5 epitope tag were used for the detection of $(Tb)_2$ and $(Tb')_2$ dimers, respectively. The experiment was done a total of four times, and the average fraction dimer is graphed below each lane. *D*, disulfide cross-link formation in heterodimeric *Tb*/*Tb′* peripheral stalks was detected using a Nickel-resin purification assay as previously described (22). Samples KM2/pSBC123/pSBC125 (Tb_{A83C}/Tb'_{A83C}), KM2/pSBC123/pSBC126 (Tb_{A83C}/Tb'_{A90C}), KM2/pSBC124/pSBC125 (Tb_{A90C}/Tb'_{A83C}), and KM2/pSBC124/pSBC126 (Tb_{A90C}/Tb'_{A90C}) were prepared and cross-linked as before. Each sample was then solubilized and purified over a high capacity nickel chelate affinity matrix to retain only F_1F_0 complexes containing at least one histidine tag. A total of 10% of the protein retained by the high capacity nickel chelate affinity matrix resin was analyzed by Western blot using an antibody against the V5 epitope tag. The average fraction dimer is graphed below each lane ($n = 8$).

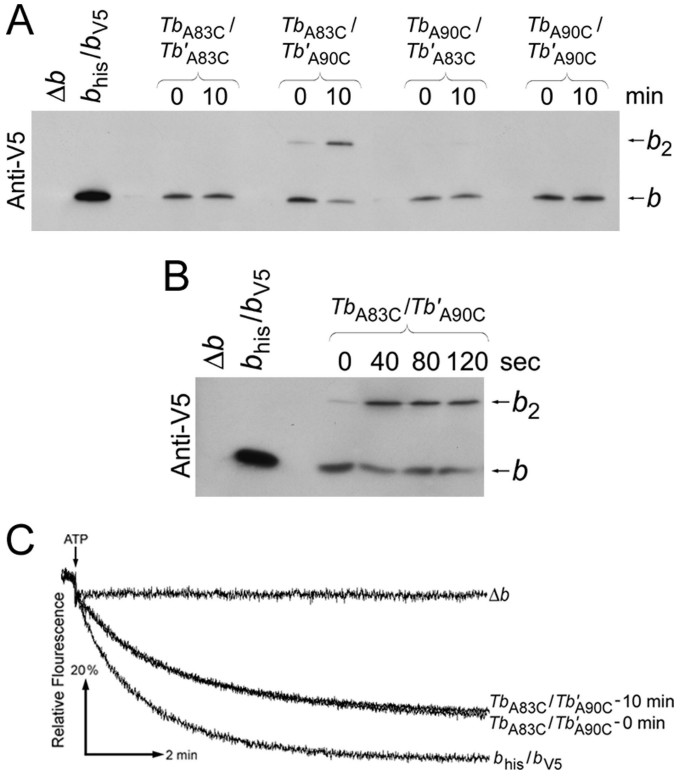

FIGURE 5. **Disulfide cross-link formation at low Cu^{2+} concentration in F_1F_0 ATP synthase peripheral stalks composed of chimeric *Tb* and *Tb′* subunits.** *A*, the membranes were prepared from strains KM2/pSBC123/pSBC125 (Tb_{A83C}/Tb'_{A83C}), KM2/pSBC123/pSBC126 (Tb_{A83C}/Tb'_{A90C}), KM2/pSBC124/pSBC125 (Tb_{A90C}/Tb'_{A83C}), and KM2/pSBC124/pSBC126 (Tb_{A90C}/Tb'_{A90C}). Each sample was cross-linked with 50 mM Cu^{2+} for 10 min and analyzed by Western blot using an antibody against the V5 epitope tag exactly as described for Fig. 2*B*. *B*, membrane sample were prepared from strain KM2/pSBC123/pSBC126 (Tb_{A83C}/Tb'_{A90C}) and cross-linked with 50 μM Cu^{2+} for increasing lengths of time. Each sample was allowed to react for the length of time specified above the Western blot before the reaction was quenched by the addition of NEM to a final concentration of 5 mM. *C*, membranes prepared from strain KM2/pSBC123/pSBC126 (Tb_{A83C}/Tb'_{A90C}) were assayed for ATP-driven proton pumping activity both before and after disulfide cross-link formation using 50 μM Cu^{2+} for 10 min. The *traces* shown are individual representative results ($n = 3$).

in-register model was supported by the observation of disulfide bridge formation in homodimeric *E. coli* peripheral stalks where both *b* subunits had identical cysteine substitutions. Disulfide cross-link formation was observed at multiple sites within the dimerization domain including b_{R83C}, b_{A90C}, and b_{E97C}. However, it was not possible to conduct a comparable experiment to test the offset model using the wild-type *E. coli* peripheral stalk because both *b* subunits are identical and hence indistinguishable within the holoenzyme. To overcome this limitation, we employed *Tb* and *Tb′* chimeric subunits constructed by replacing residues Glu^{39}–Ile^{86} of the *E. coli b* subunit with a homologous sequence from the organism *T. elongatus* as previously described (23). The cross-links favoring the in-register arrangement were reproducible in F_1F_0 complexes containing homodimeric Tb_{A83C}, Tb_{A90C}, Tb'_{A83C} and Tb_{A90C} chimeric subunits. However, studies utilizing both polypeptides modeling the chimeric *Tb/Tb′* subunits and the chimeric subunits incorporated into intact functional F_1F_0 ATP synthases demonstrated that the chimeric subunits assume preferred positions relative to one another as dictated by the *T. elongatus* sequence. Very efficient cross-linking was observed in the $Tb_{his,A83C}/Tb'_{A90C,V5}$ heterodimeric peripheral stalk, strongly favoring a staggered conformation with the *Tb* subunit shifted in the carboxyl direction relative to *Tb′*. To use the nomenclature introduced previously (16), these results suggest that in the heterodimeric *bb′* stator stalk of cyanobacteria, the *b′* subunit preferentially assumes the b^N position, and the *b* subunit occupies the b^C position. The rapid, high yield dimer formation within holoenzyme argues that the predominant arrangement of the heterodimeric peripheral stalks is the staggered conformation. Moreover, covalently fixing the offset in place did not have any affect on the coupled activity of F_1F_0 ATPase. Therefore, the staggered parallel conformation is a viable functional structure for the peripheral stalk. The evidence from our current data set is not sufficient to be interpreted as definitive in terms of establishing either a left- or right-handed coiled coil in the peripheral stalk.

Disulfide cross-link formation induced by larger amounts of oxidizing agent produced evidence of the existence of an in-register conformation in both chimeric and wild-type peripheral stalks. The most efficient cross-link was formed between cysteines substituted at residues Ala^{90} in both cases, Tb_{A90C}/Tb'_{A90C} and ($b_{A90C,V5}$). Approximately 70% of the Tb_{A83C}/Tb'_{A90C} was very rapidly cross-linked upon exposure to Cu^{2+} in peripheral stalks in the staggered conformation (Fig. 5), but using a much higher concentration of oxidizing agent as much as 70% of the Tb_{A90C}/Tb'_{A90C} and ($b_{A90C,V5}$) peripheral stalks were also cross-linked in the in-register arrangement. Regardless of whether one assumes a left- or right-handed coiled coil, residues 83 and 90 would be located not less than 10 Å apart in the in-register conformation. Given that the average disulfide bond is only 2.2 Å, residue Tb'_{A90C} cannot be within cross-linking distance of both Tb_{A83C} and Tb_{A90C}. A model where the peripheral stalk exists in equilibrium between the staggered and in-register conformations might explain the observation that both arrangements can be detected. However, the fact that the staggered arrangement can be trapped rapidly upon treatment with far less oxidizing agent implies that this more efficient cross-link represents the predominant conformation.

An obvious concern is whether the conformations detected using the *Tb/Tb′* chimeric subunit enzymes are representative of conformations present in authentic F_1F_0 ATP synthases. There are several lines of evidence that address this contention. First, the *Tb* and *Tb′* subunits were efficiently assembled into the *E. coli* F_1F_0 ATP synthase *in vivo* (23). Second, the chimeric enzymes displayed fully coupled ATP-driven proton pumping activity, which requires that the chimeric subunits not only be incorporated into F_1F_0 but also be positioned such that they can participate in all of the protein-protein interactions within both F_1 and F_0 needed for a functional enzyme complex. Finally, the cross-linking results for the *E. coli* $(b_{A83C,V5})_2$ and $(b_{A90C,V5})_2$ peripheral stalks are nearly identical to those of the chimeric Tb_{A83C}/Tb'_{A83C} and Tb_{A90C}/Tb'_{A90C} peripheral stalks, suggesting that the conformation of the chimeric peripheral stalk may be the same as the wild-type peripheral stalk. Therefore, it seems that the most reasonable interpretation is that the properties of the chimeric *Tb* and *Tb′* subunits accurately reflect the normal functions of a wild-type *b* subunit. A conclusive proof

for the staggered conformation awaits similar experiments conducted in a photosynthetic organism with native *b* and *b′* subunits.

Acknowledgment—We are pleased to acknowledge the excellent technical assistance of Yumin Bi.

REFERENCES

1. von Ballmoos, C., Cook, G. M., and Dimroth, P. (2008) *Annu. Rev. Biophys.* **37,** 43–64
2. Devenish, R. J., Prescott, M., and Rodgers, A. J. (2008) *Int. Rev. Cell. Mol. Biol.* **267,** 1–58
3. Nakamoto, R. K., Scanlon, J. A., and Al-Shawi, M. K. (2008) *Arch. Biochem. Biophys.* **476,** 43–50
4. Dimroth, P., von Ballmoos, C., and Meier, T. (2006) *EMBO Rep.* **7,** 276–282
5. Abrahams, J. P., Leslie, A. G., Lutter, R., and Walker, J. E. (1994) *Nature* **370,** 621–628
6. Weber, J. (2006) *Biochim. Biophys. Acta* **1757,** 1162–1170
7. Weber, J. (2007) *Trends. Biochem. Sci.* **32,** 53–56
8. Walker, J. E., and Dickson, V. K. (2006) *Biochim Biophys. Acta* **1757,** 286–296
9. Revington, M., McLachlin, D. T., Shaw, G. S., and Dunn, S. D. (1999) *J. Biol. Chem.* **274,** 31094–31101
10. Zaida, T., Hornung, T., Volkov, O., Hoffman, A., Pandey, S., Wise, J., and Vogel, P. (2008) *J. Bioenerg. Biomembr.* **40,** 551–559
11. Steigmiller, S., Börsch, M., Gräber, P., and Huber, M. (2005) *Biochim. Biophys. Acta* **1708,** 143–153
12. Dmitriev, O., Jones, P. C., Jiang, W., and Fillingame, R. H. (1999) *J. Biol. Chem.* **274,** 15598–15604
13. Del Rizzo, P. A., Bi, Y., Dunn, S. D., and Shilton, B. H. (2002) *Biochemistry* **41,** 6875–6884
14. Priya, R., Tadwal, V. S., Roessle, M. W., Gayen, S., Hunke, C., Peng, W. C., Torres, J., and Grüber, G. (2008) *J. Bioenerg. Biomembr.* **40,** 245–255
15. Wood, K. S., and Dunn, S. D. (2007) *J. Biol. Chem.* **282,** 31920–31927
16. Del Rizzo, P. A., Bi, Y., and Dunn, S. D. (2006) *J. Mol. Biol.* **364,** 735–746
17. Hornung, T., Volkov, O. A., Zaida, T. M., Delannoy, S., Wise, J. G., and Vogel, P. D. (2008) *Biophys. J.* **94,** 5053–5064
18. Wise, J. G., and Vogel, P. D. (2008) *Biophys. J.* **94,** 5040–5052
19. Rodgers, A. J., Wilkens, S., Aggeler, R., Morris, M. B., Howitt, S. M., and Capaldi, R. A. (1997) *J. Biol. Chem.* **272,** 31058–31064
20. Rodgers, A. J., and Capaldi, R. A. (1998) *J. Biol. Chem.* **273,** 29406–29410
21. McLachlin, D. T., and Dunn, S. D. (1997) *J. Biol. Chem.* **272,** 21233–21239
22. Grabar, T. B., and Cain, B. D. (2003) *J. Biol. Chem.* **278,** 34751–34756
23. Claggett, S. B., Grabar, T. B., Dunn, S. D., and Cain, B. D. (2007) *J. Bacteriol.* **189,** 5463–5471
24. McCormick, K. A., and Cain, B. D. (1991) *J. Bacteriol.* **173,** 7240–7248
25. Meselson, M., and Yuan, R. (1968) *Nature* **217,** 1110–1114
26. Dunn, S. D., and Chandler, J. (1998) *J. Biol. Chem.* **273,** 8646–8651
27. Dykxhoorn, D. M., St Pierre, R., and Linn, T. (1996) *Gene.* **177,** 133–136
28. Caviston, T. L., Ketchum, C. J., Sorgen, P. L., Nakamoto, R. K., and Cain, B. D. (1998) *FEBS Lett.* **429,** 201–206
29. Smith, P. K., Krohn, R. I., Hermanson, G. T., Mallia, A. K., Gartner, F. H., Provenzano, M. D., Fujimoto, E. K., Goeke, N. M., Olson, B. J., and Klenk, D. C. (1985) *Anal. Biochem.* **150,** 76–85
30. Sorgen, P. L., Bubb, M. R., McCormick, K. A., Edison, A. S., and Cain, B. D. (1998) *Biochemistry* **37,** 923–932
31. Webb, M. R. (1992) *Proc. Natl. Acad. Sci. U. S. A.* **89,** 4884–4887
32. Gardner, J. L., and Cain, B. D. (1999) *Arch. Biochem. Biophys.* **361,** 302–308
33. Grabar, T. B., and Cain, B. D. (2004) *J. Biol. Chem.* **279,** 31205–31211
34. Sorgen, P. L., Caviston, T. L., Perry, R. C., and Cain, B. D. (1998) *J. Biol. Chem.* **273,** 27873–27878